Inorg. Chem. **2006**, *45*, 3124–3132

DNA Oxidation in Anionic Reverse Micelles: Ruthenium-Mediated Damage at Guanine in Single- and Double-Stranded DNA

Sarah E. Evans,[†] Soe Mon,[†] Robinder Singh,[†] Lev R. Ryzhkov,[§] and Veronika A. Szalai*[,†]

Department of Chemistry & Biochemistry, University of Maryland, Baltimore County, 1000 Hilltop Circle, Baltimore, Maryland 21250, and Department of Chemistry, Towson University, 8000 York Road, Towson, Maryland 21252

Received December 8, 2005

One-electron guanine oxidation in DNA has been investigated in anionic reverse micelles (RMs). A photochemical method for generating Ru^{3+} from the ruthenium polypyridyl complex tris(2-2′-bipyridine)ruthenium(II) chloride ($[Ru(bpy)_3]Cl_2$) is combined with high-resolution polyacrylamide gel electrophoresis (PAGE) to quantify piperidine-labile guanine oxidation products. As characterized by emission spectroscopy of $Ru(bpy)_3^{2+}$, the addition of DNA to RMs containing $Ru(bpy)_3^{2+}$ does not perturb the environment of $Ru(bpy)_3^{2+}$. The steady-state quenching efficiency of $Ru(bpy)_3^{2+*}$ with $K_3[Fe(CN)_6]$ in buffer solution is approximately 2-fold higher than that observed in RMs. Consistent with the difference in quenching efficiency in the two media, a 1.5-fold higher yield of piperidine-labile damage products as monitored by PAGE is observed for duplex oligonucleotide in buffer vs RMs. In contrast, a 13-fold difference in the yield of PAGE-detected G oxidation products is observed when single-stranded DNA is the substrate. Circular dichroism spectra showed that single-stranded DNA undergoes a structural change in anionic RMs. This structural change is potentially due to cation-mediated adsorption of the DNA phosphates on the anionic headgroups of the RMs, leading to protection of the guanine from oxidatively generated damage.

Introduction

Cells contain high concentrations of biomolecules, making their interiors densely packed. This macromolecular crowding affects the rates of enzymatic reactions, association processes, and macromolecular structure. The effects of biomolecular crowding on protein−nucleic acid interactions,[1−4] protein refolding,[5] and protein assembly[6] have all been investigated with the goal of uncovering the biophysical phenomena that control differences between dilute solution experiments and in vivo conditions. Oxidatively generated damage or modification of guanines in DNA is a process important in mutagenesis and cancer in vivo; however, most experimental measurements on the rates and yields of these reactions have been carried out in dilute solutions.[7−9] Other studies have assessed DNA damage in chromatin or nucleosomes with ionizing radiation,[10−17] metal ions in the presence of reductants,[18−20] and chemotherapeutics.[21−24] Condensation of duplex DNA by spermine[25−34] or spermine derivatives[35]

* To whom correspondence should be addressed, E-mail: vszalai@umbc.edu.

[†] University of Maryland, Baltimore County.

[§] Towson University.

(1) Murphy, L. D.; Zimmerman, S. B. *Biochim. Biophys. Acta* **1994**, *1219*, 277.
(2) Record, M. T., Jr.; Courtenay, E. S.; Cayley, S.; Guttman, H. J. *Trends Biochem. Sci.* **1998**, *23*, 190.
(3) Reddy, M. K.; Weitzel, S. E.; Daube, S. S.; Jarvis, T. C.; von Hippel, P. H. *Methods Enzymol.* **1995**, *262*, 466.
(4) Wenner, J. R.; Bloomfield, V. A. *Biophys. J.* **1999**, *77*, 3234.
(5) van den Berg, B.; Wain, R.; Dobson, C. M.; Ellis, R. J. *EMBO J.* **2000**, *19*, 3870.
(6) Minton, A. P. *Curr. Opin. Struct. Biol.* **2000**, *10*, 34.
(7) Burrows, C. J.; Muller, J. G. *Chem. Rev.* **1998**, *98*, 1109.
(8) Hall, D. B.; Holmlin, R. E.; Barton, J. K. *Nature* **1996**, *384*, 731.
(9) Stemp, E. D. A.; Arkin, M. R.; Barton, J. K. *J. Am. Chem. Soc.* **1997**, *119*, 2921.
(10) Nygren, J.; Ljungman, M.; Ahnstrom, G. *Int. J. Radiat. Biol.* **1995**, *68*, 11.
(11) Ljungman, M. *Radiat. Res.* **1991**, *126*, 58.
(12) Ljungman, M.; Hanawalt, P. C. *Mol. Carcinog.* **1992**, *5*, 264.
(13) Chiu, S. M.; Xue, L. Y.; Friedman, L. R.; Oleinick, N. L. *Biochemistry* **1995**, *34*, 2653.
(14) Chiu, S. M.; Xue, L. Y.; Friedman, L. R.; Oleinick, N. L. *Radiat. Res.* **1992**, *129*, 184.
(15) Chiu, S. M.; Friedman, L. R.; Xue, L. Y.; Oleinick, N. L. *Int. J. Radiat. Biol.* **1986**, *12*, 1529.
(16) Chiu, S. M.; Oleinick, N. L. *Int. J. Radiat. Biol.* **1982**, *41*, 71.
(17) Chiu, S. M.; Oleinick, N. L.; Friedman, L. R.; Stambrook, P. J. *Biochim. Biophys. Acta* **1982**, *699*, 15.
(18) Liang, Q.; Dedon, P. C. *Chem. Res. Toxicol.* **2001**, *14*, 416.
(19) Hayes, J. J.; Tullius, T. D.; Wolffe, A. P. *Proc. Natl. Acad. Sci. U.S.A.* **1990**, *87*, 7405.

10.1021/ic0521022 CCC: $33.50
Published on Web 03/07/2006

decreases the levels of one-electron oxidized G products[25,35] or oxidative products generated by γ-radiation,[26−34] indicating that the environment of DNA is linked closely to the amount and type of damage. We are interested in DNA damage and the oxidative reactions of G in reverse micelles (RMs), in which DNA has been proposed to adopt a condensed structure similar to that observed in vivo.[36−38]

Solutions of RMs consist of a surfactant, a hydrocarbon solvent, and water.[37] Proper control of the ratios of components produces optically transparent solutions containing water pools with sizes and properties governed by the water: surfactant ratio ($w_0 = [H_2O]/[\text{surfactant}]$).[37] Interfacial water in the interior of RMs has been proposed to be similar in physical properties to those of water present in biological membranes.[39] At w_0 values less than 10, up to 12 water molecules interact with the headgroups of anionic surfactants and their Na^+ counterions, resulting in "structured" water.[39] At w_0 values greater than 20, the water pools contain mostly free water, whereas w_0 values between 10 and 20 represent an intermediate regime.[37] Nucleic acids, both DNA and RNA, can be trapped inside the water pools of RMs.[38] Circular dichroism spectra of DNA entrapped in RMs composed of anionic surfactants at $w_0 = 14-22$ suggest that the DNA is highly compact,[38] a state potentially similar to that in the nucleus of cells.[40]

Previous investigations of DNA oxidation in dilute aqueous environments have shown that Ru^{3+} polypyridyl complexes oxidize guanines in DNA.[9,41−43] Although Ru^{3+} is not implicated in physiological G oxidation, it provides an excellent model of in vivo one-electron oxidation of DNA.[7] In one method known as the "flash-quench" process (Scheme 1),[9] electronic excitation of Ru^{2+} followed by oxidative quenching of $Ru^{2+}*$ to generate Ru^{3+} leads to one-electron oxidation of G and formation of the guanine radical cation ($G^{\bullet+}$).[44] Deprotonation of $G^{\bullet+}$ generates the neutral radical ($G^{\bullet}$), which reacts with O_2 to produce piperidine-labile oxidation products. The guanine radical cation also can react with water to generate 8-oxo-7,8-dihydroguanine (8OG) via a second oxidation reaction. Reduction of Ru^{3+} or oxidized guanines can occur by recombination reactions with the reduced quencher. The rates of G oxidation by tris(2,2′-bipyridine)ruthenium(III), $Ru(bpy)_3^{3+}$, in dilute solution are well-established,[42,45−47] making the reaction a useful probe of DNA oxidation in RMs. In addition to being an effective oxidant of DNA, spectroscopic information on $Ru(bpy)_3^{2+}$ in RMs is available.[48,49]

Scheme 1. Flash-quench of $Ru(bpy)_3^{2+}$ with DNA

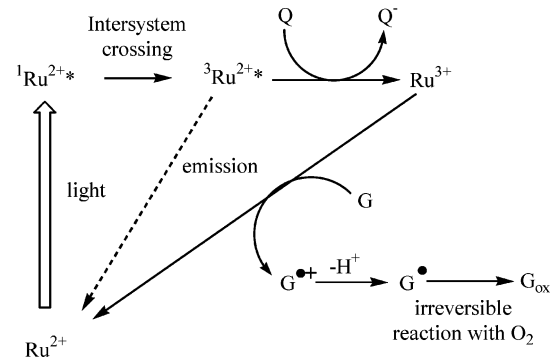

In general, yields of photogenerated products increase when photoionization is initiated in organized media.[50,51] For example, in RMs composed of sodium bis(2-ethylhexyl)-sulfosuccinate (AOT), the yields of photooxidized products depend on both the size of the RMs (w_0 value) and the nature of the species being oxidized (charged vs neutral and overall hydrophobicity). In an AOT RM system containing a water-soluble acceptor and donors with hydrocarbon tails, photoyields decreased as donor tail length increased because the donor was localized in the hydrocarbon solvent, farther from the acceptor in the water pool. When both the donor (photoactive species) and acceptor (quencher) are soluble exclusively in the water pools, the rate constant for quenching of the donor excited state increases by a factor of 400 over that for a hydrocarbon-soluble donor paired with the same water-soluble quencher.[52] On the basis of these results, we expected oxidatively generated damage at G in RMs to be more extensive than that observed in a dilute buffer solution.

(20) Dixon, W. J.; Hayes, J. J.; Levin, J. R.; Weidner, M. F.; Dombrowski, B. A.; Tullius, T. D. *Methods Enzymol.* **1991**, *208*, 380.
(21) Liang, Q.; Choi, D.-J.; Dedon, P. C. *Biochemistry* **1997**, *36*, 12653.
(22) Wu, J.; Xu, J.; Dedon, P. C. *Biochemistry* **1999**, *38*, 15641.
(23) Yu, L.; Goldberg, I. H.; Dedon, P. C. *J. Biol. Chem.* **1994**, *269*, 4144.
(24) Yu, L.; Salzberg, A. A.; Dedon, P. C. *Bioorg. Med. Chem.* **1995**, *3*, 729.
(25) Hosford, M. E.; Muller, J. G.; Burrows, C. J. *J. Am. Chem. Soc.* **2004**, *126*, 9540.
(26) Douki, T.; Bretonniere, Y.; Cadet, J. *Radiat. Res.* **2000**, *153*, 29.
(27) Chiu, S. M.; Oleinick, N. L. *Radiat. Res.* **1998**, *149*, 543.
(28) Khan, A. U.; Di Mascio, P.; Medeiros, M. H.; Wilson, T. *Proc. Natl. Acad. Sci. U.S.A.* **1992**, *89*, 11428.
(29) Khan, A. U.; Mei, Y. H.; Wilson, T. *Proc. Natl. Acad. Sci. U.S.A.* **1992**, *89*, 11426.
(30) Spotheim-Maurizot, M.; Ruiz, S.; Sabattier, R.; Charlier, M. *Int. J. Radiat. Biol.* **1995**, *68*, 571.
(31) Newton, G. L.; Aguilera, J. A.; Ward, J. F.; Fahey, R. C. *Radiat. Res.* **1996**, *145*, 776.
(32) Newton, G. L.; Aguilera, J. A.; Ward, J. F.; Fahey, R. C. *Radiat. Res.* **1997**, *148*, 272.
(33) Newton, G. L.; Ly, A.; Tran, N. Q.; Ward, J. F.; Milligan, J. R. *Int. J. Radiat. Biol.* **2004**, *80*, 643.
(34) Warters, R. L.; Newton, G. L.; Olive, P. L.; Fahey, R. C. *Radiat. Res.* **1999**, *151*, 354.
(35) Cao, H.; Schuster, G. B. *Bioconjugate Chem.* **2005**, *16*, 820.
(36) Pietrini, A. V.; Luisi, P. L. *Biochim. Biophys. Acta* **2002**, *1562*, 57.
(37) Luisi, P. L., Straub, B., Eds. *Reverse Micelles*; Plenum Press: New York, 1984.
(38) Imre, V. E.; Luisi, P. L. *Biochem. Biophys. Res. Commun.* **1982**, *107*, 538.
(39) Jain, T. K.; Varshney, J.; Maitra, A. *J. Phys. Chem.* **1989**, *93*, 7409.
(40) Voet, D.; Voet, J. G. *Biochemistry*, 2nd ed.; John Wiley & Sons: New York, 1995.
(41) Arkin, M. R.; Stemp, E. D. A.; Pulver, S. C.; Barton, J. K. *Chem. Biol.* **1997**, *4*, 389.
(42) Johnston, D. H.; Glasgow, K. C.; Thorp, H. H. *J. Am. Chem. Soc.* **1995**, *117*, 8933.
(43) Neyhart, G. A.; Cheng, C.-C.; Thorp, H. H. *J. Am. Chem. Soc.* **1995**, *117*, 1463.
(44) Schiemann, O.; Turro, N. J.; Barton, J. K. *J. Phys. Chem. B* **2000**, *104*, 7214.
(45) Johnston, D. H.; Welch, T. W.; Thorp, H. H. Electrochemically Activated Nucleic Acid Oxidation. In *Metal Ions in Biological Systems*; Sigel, A., Sigel, H., Eds.; Marcel Dekker: New York, 1996; Vol. 33; p 297.
(46) Szalai, V. A.; Thorp, H. H. *J. Phys. Chem. B* **2000**, *104*, 6851.
(47) Yang, I. V.; Thorp, H. H. *Inorg. Chem.* **2000**, *39*, 4969.
(48) Atik, S. S.; Thomas, J. K. *J. Am. Chem. Soc.* **1981**, *103*, 3543.
(49) Handa, T.; Sakai, M.; Nakagaki, M. *J. Phys. Chem.* **1986**, *90*, 3377.
(50) Baglioni, P.; Nakamura, H.; Kevan, L. *J. Phys. Chem.* **1991**, *95*, 3856.
(51) Nakamura, H.; Baglioni, P.; Kevan, L. *J. Phys. Chem.* **1991**, *95*, 1480.
(52) Atik, S. S.; Thomas, J. K. *J. Phys. Chem.* **1981**, *85*, 3921.

Our work combines the investigation of DNA reactivity with that of DNA structure in RMs. Using ruthenium polypyridyl complexes, quencher, and DNA, we have probed the yield of G oxidation in AOT RMs with $w_0 = 18$. Under comparable illumination conditions in RMs and buffer solution, we observe similar yields of oxidatively generated products for a duplex oligonucleotide, as detected by piperidine-induced strand scission reactions. In contrast, a 13-fold higher yield of piperidine-labile G oxidation products is observed for a single-stranded oligonucleotide in buffer solution vs RMs. We ascribe the low yield of oxidatively generated products observed for a single-stranded oligonucleotide in RMs to the change in structure of the single-stranded oligonucleotide in this environment.

Experimental Section

Reagents. $Ru(bpy)_3Cl_2$ was purchased from Aldrich (Milwaukee, WI) and recrystallized from water/acetone. The extinction coefficient of $Ru(bpy)_3^{2+}$ at 452 nm in water is 14 600 M^{-1} cm^{-1}.[53] Bis(bipyridine)dipyridophenazine ruthenium(II) hexafluorophosphate ($[Ru(bpy)_2dppz](PF_6)_2$) was a gift from Dr. Rebecca Holmberg and Dr. H. Holden Thorp at the University of North Carolina at Chapel Hill. The chloride salt of $[Ru(bpy)_2dppz](PF_6)_2$ was generated by dissolving the complex in acetone and adding a concentrated solution of tetrabutylammonium chloride in acetone; the chloride salt of the complex is insoluble in acetone. The extinction coefficient for $Ru(bpy)_2dppz^{2+}$ at 444 nm in water is 16 100 M^{-1} cm^{-1}.[54] Herring testes DNA and sodium bis(2-ethylhexyl)sulfosuccinate (AOT) were purchased from Sigma (St. Louis, MO). Water was deionized and polished using a MilliQ water purification system (ϵ > 18 mΩ). Solutions of 40% acrylamide: bis(acrylamide) in a 29:1 ratio were purchased from National Diagnostics (Atlanta, GA). Tetramethylethylenediamine (TEMED), ammonium persulfate, mercaptoethanol, ethylenediamine tetraacetic acid disodium salt (Na_2EDTA), and potassium ferricyanide ($K_3[Fe(CN)_6]$) were supplied by Acros (Morris Plains, NJ). Heptane, isooctane, methanol, tris(hydroxymethyl)aminomethane (TRIS), boric acid, and urea were purchased from Fisher (Pittsburgh, PA). Piperidine and dimethyl sulfate were purchased from Aldrich (Milwaukee, WI). Oligonucleotides were supplied by the W. M. Keck Facility at Yale University, and concentrations were determined spectrophotometrically using a Jasco V-560 dual-beam UV−vis spectrometer. The extinction coefficient of herring testes DNA (in nucleotides) is 6600 M^{-1} cm^{-1}.[55] The oligonucleotide 5′-d[GATGAGAGTTAGTGATGAGTG]-3′ (**1**) extinction coefficient was calculated using the nearest-neighbor approximation[56] to be 190.2 mM^{-1} cm^{-1}. Solutions of AOT in heptane were prepared and passed through a Whatman 0.5 micron PTFE filter prior to use. Volumes of AOT in heptane for RM samples were measured with Hamilton gas-tight glass syringes.

General Radiolabeling and Polyacrylamide Gel Electrophoresis (PAGE). Oligonucleotides were piperidine-treated and gel purified in a 20% polyacrylamide gel containing 7 M urea according to standard procedures.[57] The purified oligonucleotide was radiolabeled with [γ-^{32}P]-ATP (10 mCi/mL, Perkin-Elmer Life Sciences, Boston, MA) using T4 polynucleotide kinase (Invitrogen, Carlsbad, CA), as previously described.[58] Double-stranded DNA was generated by combining a 1:1.1 ratio of **1** with its gel-purified Watson−Crick complement in buffer solution. After ^{32}P-radiolabeled **1** was added, the solution was heated to 95 °C for 5 min and then allowed to cool to room temperature over 2 h. Denaturing PAGE was performed at 50 °C on 20% polyacrylamide gels containing 7 M urea. Electrophoresis running buffer was 1× TBE and was prepared from a 10× TBE stock containing 0.89 M Tris, 20 mM Na_2EDTA, and 0.89 M boric acid, pH 8.3. All gels were wrapped and placed on a phosphor screen, exposed for 1 h for quantification of band intensities, scanned on an Amersham Biosciences Typhoon 9200 instrument, and analyzed using ImageQuaNT software.

Guanine Oxidation Reactions. A stock solution of ^{32}P-radiolabeled single-stranded oligonucleotide was prepared by combining ^{32}P-radiolabeled **1**, 1.57 mM unlabeled **1**, and 50 mM NaP_i, pH 7, so that the final concentrations in each sample were 10 μM **1** and 10 mM NaP_i. A stock solution of ^{32}P-radiolabeled double-stranded oligonucleotide **1** was prepared as described above using a stock solution of 1.27 mM unlabeled **1**, 2.00 mM complement, and 250 mM NaP_i, pH 7, to give final concentrations of 10 μM duplex **1** and 10 mM NaP_i. NaP_i concentrations for both single- and double-stranded solutions were calculated on the basis of total water content in the samples, whereas those for all other components were calculated on the basis of total sample volume. Oxidative cleavage experiments were performed by combining stock solutions of ^{32}P-radiolabeled single-stranded **1** with the appropriate amounts of solutions of 5 mM $Ru(bpy)_3^{2+}$ and 50 mM $Fe(CN)_6^{3-}$ in water to give the final concentrations given in the figure legends. The concentrations of the $Ru(bpy)_3^{2+}$ stock solutions were confirmed spectrophotometrically. The final sample volume was adjusted to 50 μL by the addition of water. For RM samples at $w_0 = 18$ containing $Ru(bpy)_3^{2+}$ and quencher, 46 μL of a 0.2 M AOT in heptane solution was combined with 2.2 μL of ^{32}P-radiolabeled **1** stock solution and 0.5 μL of $Ru(bpy)_3^{2+}$ and $Fe(CN)_6^{3-}$ stock solutions or water to give a final volume of 49.2 μL. Photolysis was performed for 10 min at room temperature with a 300 W Hg lamp (Oriel) with a UV cutoff filter (<350 nm). Samples were ethanol-precipitated twice, piperidine treated (0.7 M piperidine, 90 °C for 30 min), and prepared for PAGE as described previously.[58] Positions of guanines were determined by Maxam−Gilbert sequencing of ^{32}P-radiolabeled **1**.[58] Illuminated samples containing the ruthenium polypyridyl complex and quencher were run in triplicate on each gel. The average G cleavage ratio for multiple samples containing the same ruthenium polypyridyl complex concentration was calculated from the average volume intensity for all of the G oxidation products for each sample. Errors given represent the standard deviation between the average G cleavage ratios for each sample at a fixed ruthenium polypyridyl complex concentration unless otherwise noted. Each gel was run at least three times to confirm the reproducibility of results.

Emission Spectroscopy. Emission spectra of samples containing $Ru(bpy)_3^{2+}$ (λ_{ex} = 452 nm) and $Ru(bpy)_2dppz^{2+}$ (λ_{ex} = 444 nm) were collected on a Jobin-Yvon Fluoromax-2 fluorometer. Emission spectra were collected from 500 to 800 nm with either 1 or 2 nm increments, intervals of 0.1 or 0.5 s, and slit widths of 2 or 5 nm. The photomultiplier tube (PMT) correction file supplied by the manufacturer was not applied to spectra shown in the figures. Spectra were collected on samples prepared in duplicate or triplicate.

(53) Kalyanasundaram, K. *Photochemistry of Polypyridine and Porphyrin Complexes*; Academic Press: London, 1992.
(54) Amouyal, E.; Homsi, A. *J. Chem. Soc., Dalton Trans.* **1990**, 1841.
(55) Sigma-Aldrich Technical Support 2000.
(56) Borer, P. N. *Handbook of Biochemistry and Molecular Biology*, 3rd ed.; CRC Press: Cleveland, OH, 1975.
(57) Maniatis, T.; Fritsch, E. F.; Sambrook, J. *Molecular Cloning: A Laboratory Manual*, 2nd ed.; Cold Spring Harbor Press: Plainview, NY, 1989.
(58) Szalai, V. A.; Thorp, H. H. *J. Am. Chem. Soc.* **2000**, *122*, 4524.

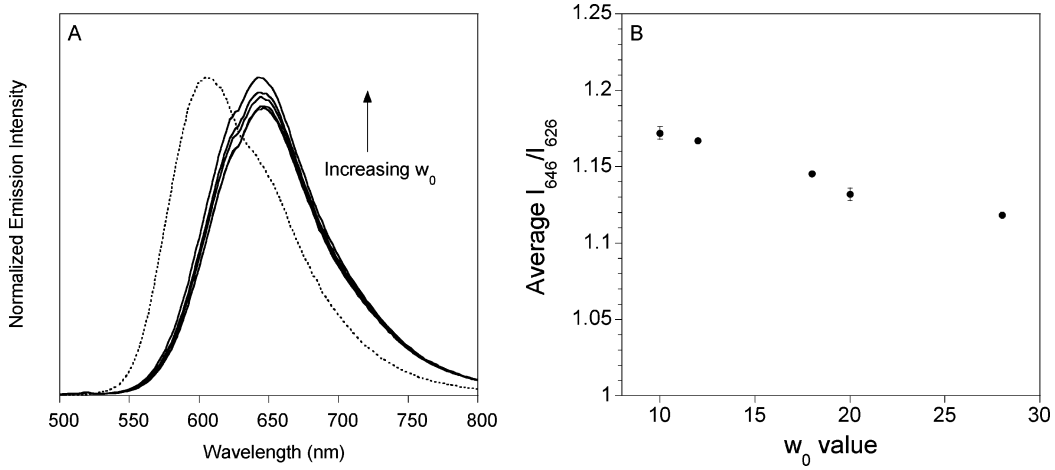

Figure 1. (a) Change in the steady-state emission spectrum intensity of 50 μM $Ru(bpy)_3^{2+}$ as a function of the w_0 value (w_0 = 10, 12, 18, 20, 28) in AOT RMs. The emission spectrum of $Ru(bpy)_3^{2+}$ in buffer is also shown (dashed line). Spectra were normalized to show the change in spectral shape; spectra collected for RM samples are normalized to the w_0 = 28 spectrum. (b) Variation in the ratio of the $Ru(bpy)_3^{2+}$ emission intensities in RMs at 646 and 626 nm as a function of the w_0 value.

Reported errors for the average emission intensities are either the range of values (duplicate measurements) or the standard deviation (triplicate measurements).

Circular Dichroism Spectroscopy. Circular dichroism (CD) measurements of **1**, duplex **1**, single- and double-stranded herring testes DNA in buffer solution, and AOT RMs were collected with 0.3 cm path length quartz cuvettes using a Jasco circular dichroism spectropolarimeter, model J-715. The following instrumental parameters were used: wavelength range, 240−400 nm; scan speed, 50 nm/min; bandwidth, 1.0 nm; response time, 1 s. The CD spectra were the average of three scans; comparable background scans without DNA were collected, averaged, and subtracted from the scans collected for solutions containing DNA. AOT stock solutions (0.05 M) were prepared in isooctane.[23] Samples containing single- or double-stranded oligonucleotides were prepared to give strand or duplex final concentrations of 10 μM in buffer solution and RMs (w_0 = 18.5). Single-stranded herring testes DNA was prepared by heating a stock solution of DNA at 95 °C for 15 min followed by immediate cooling of the solution to 4 °C. Samples containing unsheared herring testes DNA were prepared to give a final concentration of 350 μM nucleotides in buffer and RMs (w_0 = 18.5). All samples contained 10 mM NaP_i, pH 7, calculated on the basis of the volume of water in the samples; DNA concentrations were calculated on the basis of the total sample volume. For spectra of herring testes DNA collected in the presence of 50 μM $Ru(bpy)_3^{2+}$, the wavelength range was 210−600 nm and all other parameters were the same.

Results

Steady-state emission spectra of $Ru(bpy)_3^{2+}$ are sensitive to the size and interior components of the RMs.[49,59] In the experiments below, the concentration of $Ru(bpy)_3^{2+}$ in buffered water and in RMs was the same and was calculated on the basis of the total sample volume rather than the total aqueous volume because direct comparison of optical measurements is possible only if equivalent total concentrations of chromophore are employed. The steady-state emission spectrum of $Ru(bpy)_3^{2+}$ in water differs in intensity from that recorded in AOT RMs (Figure 1a). The ratio of the intensities at 646 nm for $Ru(bpy)_3^{2+}$ in buffered water and in RMs was about 1.5:1. The largest component of the emission spectrum in buffer solution has λ_{max} = 606 nm. In the same spectrum, a shoulder with λ_{max} = 646 nm is also present. In AOT RMs, the emission spectrum of $Ru(bpy)_3^{2+*}$ has features at 646 and 626 nm. The ratio of the intensities of these two peaks in RMs varies slightly as a function of the w_0 value (Figure 1b). We used this change in the emission intensity ratio to approximate the size of the RMs when they contain DNA (see below).

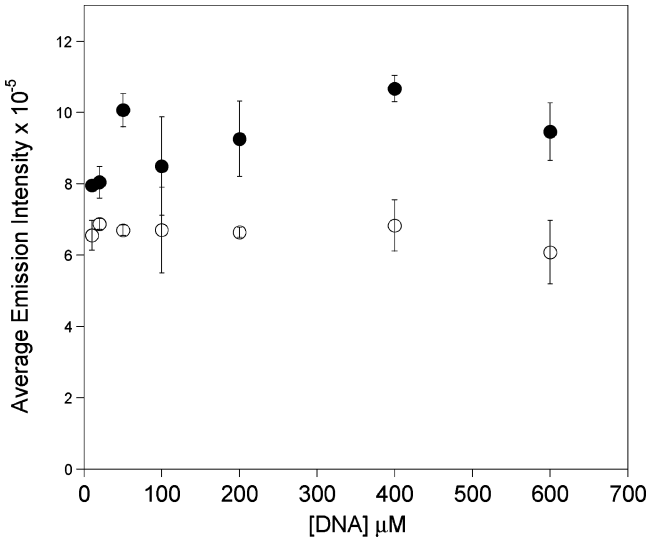

Figure 2. Change in the emission intensity of $Ru(bpy)_3^{2+}$ at 646 nm in RMs as a function of the herring testes DNA concentration. The open symbols are for w_0 = 10 and the closed symbols are for w_0 = 28 RMs.

As w_0 was increased, the ruthenium emission intensity at 646 nm in RMs increased slightly. Absorbance spectra of the same samples show no corresponding change in the absorbance intensity at 452 nm, the excitation wavelength for the emission experiments.

At fixed w_0 values, the ruthenium emission intensity did not change as the concentration of herring testes DNA increased from 10 to 600 μM nucleotides (Figure 2), and the general shape of the $Ru(bpy)_3^{2+}$ steady-state emission

(59) Meisel, D.; Matheson, M. S.; Rabani, J. *J. Am. Chem. Soc.* **1978**, *100*, 117.

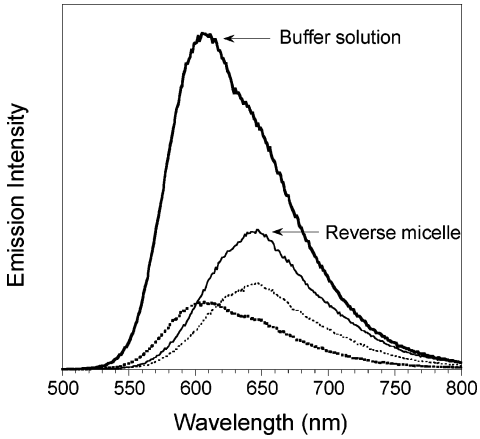

Figure 3. Emission spectra of 50 μM $Ru(bpy)_3^{2+}$ in 10 mM NaP_i, pH 7, buffer solution (bold lines) or in $w_0 = 18$ RMs containing 10 mM NaP_i, pH 7 (thin lines). Spectra of both types of samples containing 500 μM $Fe(CN)_6^{3-}$ quencher are also shown (dashed lines).

spectrum does not vary. The predicted 646:626 nm emission intensity ratios for $w_0 = 10$ and 28 RMs without DNA are 1.17 and 1.12, respectively. These ratios drop to 1.14 ($w_0 = 10$) and 1.11 ($w_0 = 28$) when DNA is present and correspond to actual w_0 values of 20 and 30, indicating that the size of the RMs increases on the addition of DNA. No change in the emission intensity ratio is observed when single-stranded **1** or duplex **1** is incorporated into RMs.

Because the $Ru(bpy)_3^{2+}$ emission spectral shape is unaffected by the addition of DNA, potentially indicating that it is not associated with DNA, we attempted to use $Ru(bpy)_2dppz^{2+}$ in AOT RMs, assuming that it would bind tightly to DNA. The affinity of this complex for duplex DNA in buffer solution is $>10^6$ M^{-1}, and a steady-state emission spectrum is observed only in the presence of DNA (i.e., not in buffer solution alone).[60] Prior to the addition of duplex DNA, a $Ru(bpy)_2dppz^{2+}$ emission spectrum is observed in AOT RMs. This spectrum does not change when duplex DNA is added (see the Supporting Information, Figure S1), which signals there is no change in the environment of the complex. Our conclusion is that $Ru(bpy)_2dppz^{2+}$ does not bind to DNA in the anionic reverse micelles and instead binds to the surfactant headgroups. Recent work showing that $Os(bpy)_2dppz^{2+}$ does not intercalate into DNA in molten salts[61] substantiates this conclusion.

The amount of caged Ru^{3+} oxidant produced in samples is proportional to the decrease in the emission intensity of $Ru(bpy)_3^{2+}$* in the presence of the ferricyanide quencher (Figure 3). In buffer solution, the $Ru(bpy)_3^{2+}$* emission intensity decreased by 85−90% in the presence of a 10-fold excess of $Fe(CN)_6^{3-}$. Quenching of $Ru(bpy)_3^{2+}$* was much less efficient in AOT RMs, where quenching of about 40% by $Fe(CN)_6^{3-}$ was observed. Transient absorbance measurements on the microsecond time scale showed no appreciable buildup of Ru^{3+} oxidant in AOT RM samples containing $Ru(bpy)_3^{2+}$ and quencher (data not shown). On the basis of this information, we expected the yield of oxidatively generated products of G in AOT RMs to be smaller than that observed in buffer solution.

The extent of G oxidation in samples containing the ruthenium photooxidant $Ru(bpy)_3^{2+}$, $Fe(CN)_6^{3-}$, and DNA oligonucleotide was monitored by high-resolution polyacrylamide gel electrophoresis to reveal oxidatively generated damage at G.[58] These experiments were conducted at $w_0 = 18$ because incorporation of all of the required components produces transparent microemulsions at this volume percent water. One-electron G oxidation of single- and double-stranded **1** by $Ru(bpy)_3^{2+}$ with $Fe(CN)_6^{3-}$ was examined in buffer solution and in AOT RMs. Representative gels are in Figure 4, and average cleavage ratios for G are given in Table 1. The concentrations of single-stranded **1**, duplex **1,** photooxidant, and quencher were calculated on the basis of the total volume of the solution and not on the volume of water in the interior of the RMs. The total volume was used to calculate concentrations because the use of a photochemical reaction to initiate G oxidation chemistry requires that the absorbance of the solutions be the same so results can be cross-compared. Lanes 2−8 contain buffer samples and lanes 9−15 contain RM samples for both gels. Control lanes 2 and 9 containing **1** or duplex **1** with no additions show that no significant strand cleavage occurred in the absence of light, ruthenium photooxidant, and quencher. Similarly, nonilluminated samples in lanes 3 and 10 containing **1** or duplex **1**, $Ru(bpy)_3^{2+}$, and $Fe(CN)_6^{3-}$ showed no cleavage above the background (see Table 1).

For single-stranded **1**, significant damage to illuminated samples occurred only for those samples treated with $Ru(bpy)_3^{2+}$ and $Fe(CN)_6^{3-}$ (Table 1). Some cleavage was observed for the illuminated buffer sample containing $Fe(CN)_6^{3-}$ in lane 5, panel A, although it is not specific for G. In buffer solutions of single-stranded **1**, the 10 min illumination time, 50 μM $Ru(bpy)_3^{2+}$ and 500 μM $Fe(CN)_6^{3-}$ were sufficient to cleave almost all of the single-stranded oligonucleotide, as shown by the lack of full-length **1** at the top of lanes 6−8 in panel A. It should be noted that the cleavage ratios given in Table 1 were calculated using the parent-band intensity to normalize the intensities of each cleavage product. Because this band is depleted significantly in lanes 6−8, the cleavage ratios are only approximate values for those lanes. In contrast to buffer solution, single-stranded **1**, $Ru(bpy)_3^{2+}$, and $Fe(CN)_6^{3-}$ in RMs produced much smaller yields of piperidine-labile G oxidation products upon illumination (lanes 13−14, Table 1).

For duplex **1**, piperidine-labile lesions resulting from G oxidation occurred upon illumination of the samples containing photooxidant and quencher. Buffer solutions of duplex **1** (panel B, lanes 6−8) showed significantly less G oxidation than single-stranded **1** in buffer solution (panel A, lanes 6−8). This result is consistent with the larger rate constant for G oxidation by $Ru(bpy)_3^{3+}$ for single-stranded DNA than for double-stranded DNA in buffer solution.[26,29,46] The cleavage ratio for duplex **1** in RMs was lower than that in buffer by a factor of 1.6 (Table 1). However, cleavage ratios for single-stranded **1** and double-stranded **1** were the same within error in the RMs.

(60) Friedman, A. E.; Chambron, J.-C.; Sauvage, J.-P.; Turro, N. J.; Barton, J. K. *J. Am. Chem. Soc.* **1990**, *112*, 4960.
(61) Leone, A. M.; Hull, D. O.; Wang, W.; Thorp, H. H.; Murray, R. W. *J. Phys. Chem. A* **2004**, *108*, 9787.

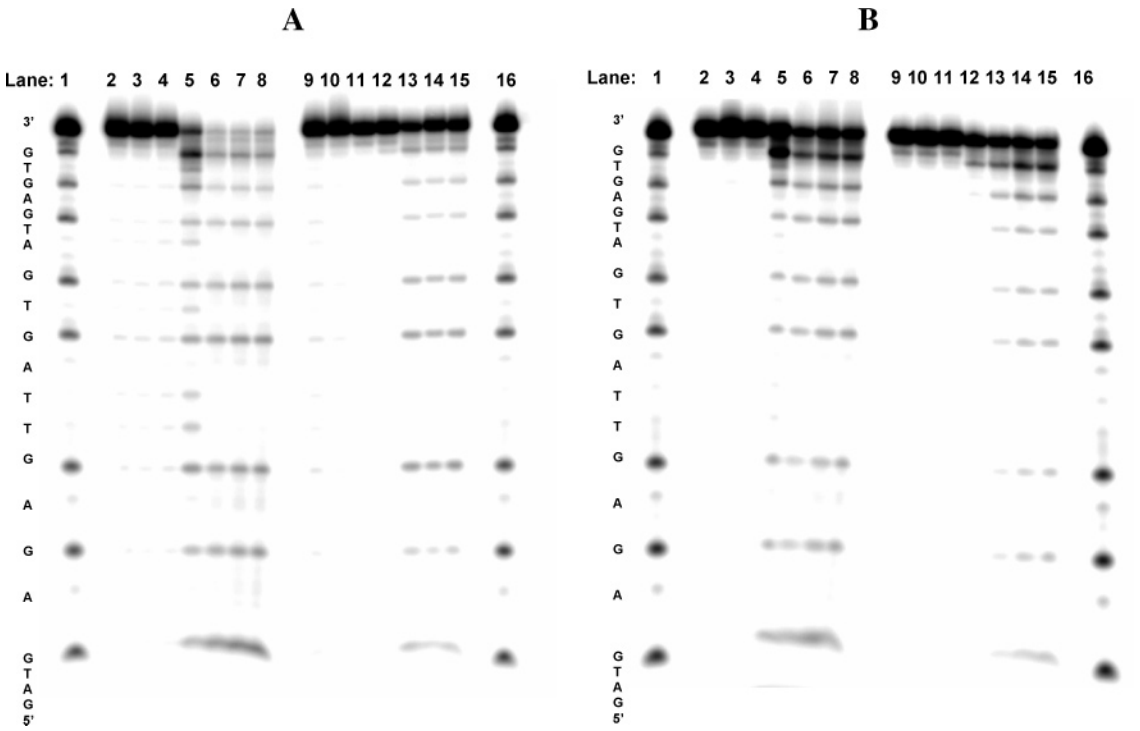

Figure 4. Phosphorimage of denaturing gels of G oxidation products formed by the oxidative quenching of $Ru(bpy)_3^{2+*}$ with (a) 10 μM **1** or (b) 10 μM duplex **1**. For both gels, lanes 2−8 contain samples in buffer solution; lanes 9−15 contain samples in RMs ($w_0 = 18$). Lanes 1 and 16 are Maxam−Gilbert G lanes. Samples in lanes 2, 3, 9, and 10 were not illuminated; samples in lanes 4−8 and 11−15 were illuminated for 10 min. Lanes 2 and 9, no additions; lanes 3 and 10, 50 μM $Ru(bpy)_3^{2+}$ and 500 μM $Fe(CN)_6^{3-}$; lanes 4 and 10, illuminated with no additions; lanes 5 and 12, illuminated with 500 μM $Fe(CN)_6^{3-}$; lanes 6−8 and 13−15, illuminated with 50 μM $Ru(bpy)_3^{2+}$ and 500 μM $Fe(CN)_6^{3-}$.

Table 1. Average Cleavage Ratios of Piperidine-Labile G Oxidation Products[a]

	cleavage ratios	
sample	buffer	RM
1	0.010 ± 0.002	0.002 ± 0.001
1 + quencher	0.149 ± 0.048	0.004 ± 0.001
1 + $Ru(bpy)_3^{2+}$ + quencher	0.528 ± 0.061[b]	0.040 ± 0.011
duplex **1**	0.005 ± 0.002	0.003 ± 0.001
duplex **1** + quencher	0.029 ± 0.011	0.009 ± 0.003
duplex **1** + $Ru(bpy)_3^{2+}$ + quencher	0.087 ± 0.004	0.054 ± 0.019

[a] Illuminated samples from Figure 4. The concentration of $Ru(bpy)_3^{2+}$ is 50 μM and the concentration of $[Fe(CN)_6]^{3-}$ is 500 μM. [b] See discussion in text.

The CD spectrum of single-stranded **1** in buffer solution is typical of single-stranded DNA.[62] Single-stranded DNA is characterized by a CD spectrum with peak maxima similar to those in duplex DNA, but with reduced peak intensities.[62] This characteristic is clearly visible for single-stranded **1** in buffer (Figure 5a) when compared to duplex **1** in buffer (Figure 5b). In contrast, the CD spectrum of single-stranded **1** in RMs is hyperchromic and hypsochromic relative to that for single-stranded **1** in buffer (Figure 5a). The absorption maximum of single-stranded **1** in RMs is decreased relative to that for single-stranded **1** in buffer solution as well (data not shown). Duplex **1** in RMs exhibits a circular dichroism spectrum that is almost identical to that collected for a solution of the same DNA in buffer solution (Figure 5B). CD spectra of herring testes DNA are similar to those previously reported for large pieces of DNA in AOT RMs (data not shown).[23] An induced CD spectrum for $Ru(bpy)_3^{2+}$ was not observed in AOT RMs containing DNA (see the Supporting Information, Figure S2).

(62) Kay, E. *Biochemistry* **1976**, *15*, 5241.

Discussion

The emission spectrum of $Ru(bpy)_3^{2+*}$ is sensitive to the environment of the metal complex, providing a useful probe of the localization of the complex in RMs.[48,49,59] Emission spectra of $Ru(bpy)_3^{2+}$ in AOT RMs are red-shifted and decreased in intensity relative to spectra of $Ru(bpy)_3^{2+}$ in buffered water solution. In RMs composed of nonionic surfactants, the emission spectrum of $Ru(bpy)_3^{2+}$ is more similar to the spectrum of $Ru(bpy)_3^{2+}$ in water as the percentage of water in the microemulsion increases.[49] The red shift in the λ_{max} of the emission spectrum for $Ru(bpy)_3^{2+}$ in RMs with low water content has been interpreted to mean that $Ru(bpy)_3^{2+}$ localizes in two distinct environments, the surface of the RM sphere created by the surfactant headgroups and the interior of the RM water pools.[49] Justification for such an interpretation is made on the basis of observed red shifts in λ_{max} for the emission spectrum of $Ru(bpy)_3^{2+}$ in alcohol solvents as the alkyl chain length increased.[59] As w_0 increases, the ratio of the peak intensities at 646 and 626 nm in the emission spectrum of $Ru(bpy)_3^{2+}$ decreases, signaling a change in the environment of the ruthenium complex as the RM size increases.

The size of the RMs changes on the addition of herring testes DNA, as evidenced by the observed decrease in the 646:626 nm emission intensity ratio. The $w_0 = 10$ RMs containing DNA have an emission intensity ratio comparable

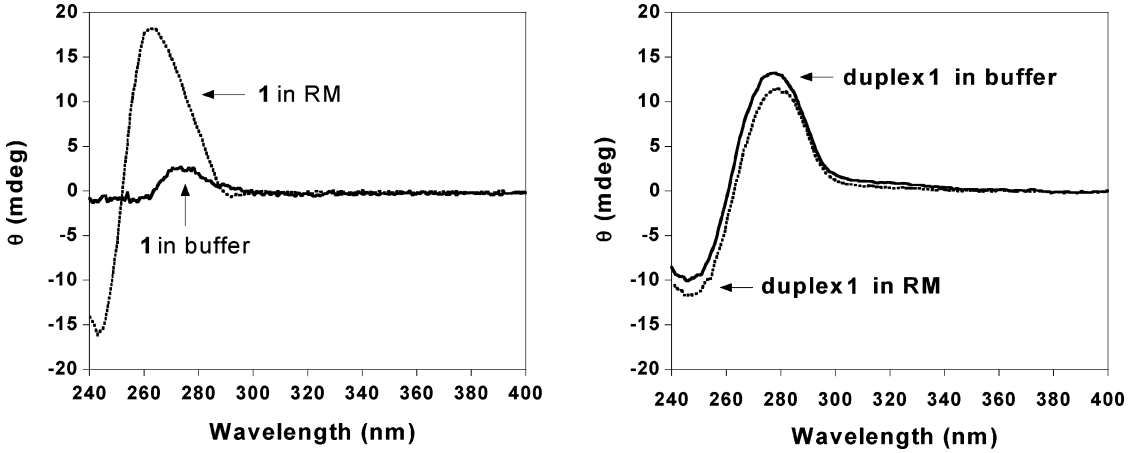

Figure 5. (a) CD spectra of 10 μM single-stranded **1** in buffer solution (solid line) and in $w_0 = 18.5$ AOT RMs (dashed line). (b) CD spectra of 10 μM duplex **1** in buffer (solid line) and in AOT $w_0 = 18.5$ RMs (dashed line).

to $w_0 = 18$ RMs without DNA, which means that the $w_0 = 10$ RMs increase in average size to accommodate DNA. Anionic RMs prepared with DNA at $w_0 = 28$ have a ratio that is almost the same as that for $w_0 = 28$ RMs prepared without DNA. This result is somewhat surprising because dynamic light-scattering measurements of solutions of $w_0 = 18.5$ anionic RMs containing large (>500 bp) DNA consist of two stable populations of RM species: one population with a 5 nm radius and the other with a 100 nm radius.[36] For herring testes DNA, the 100 nm radius form reportedly dominates the distribution; Pietrini and Luisi have proposed that this form is an aggregate of the smaller RMs.[36] If smaller-radii RMs are intact in the larger species, the $Ru(bpy)_3^{2+}$* emission intensity ratio in $w_0 = 28$ RM solutions should not change on the addition of DNA, which is the result we observe. For **1** (single-stranded or duplex), no change in RM size at any w_0 value was indicated on the addition of DNA, consistent with the close match between the length of duplex **1** (approximately 70 Å) and the diameter of $w_0 = 18.5$ RMs (approximately 80 Å).[63]

For G oxidation effected by ruthenium photochemistry to be feasible in RMs, the quenching efficiency of $Ru(bpy)_3^{2+}$* to create the Ru^{3+} oxidant must be nonzero. A previous study demonstrated that the quenching efficiency of $Ru(bpy)_3^{2+}$* by $Fe(CN)_6^{3-}$ in AOT RMs has a parabolic dependence on the size of the water pools, with maximal quenching efficiency of about 70% observed at $w_0 = 22$.[48] The same authors report that as w_0 increases, the rate constant for quenching decreases.[48] The change in quenching efficiency as a function of the w_0 value was ascribed to changes in the nature of the water pools. At w_0 values less than 10, mobility in the water pools is restricted because of the rigidity of the water associated with the surfactant headgroups and counterions.[37,48] Thus, inside smaller water pools, the collisional frequency of the probe with the quencher is decreased, which explains the low quenching efficiency. At w_0 values between 10 and 30, the water pools are large enough to permit diffusion of ions in the interior of the RMs, and the quenching efficiency increases. In contrast, in larger water pools ($w_0 > 30$), quenching efficiency decreases because the local concentrations of reactants drop because of effective dilution. We find no change in the quenching efficiency of $Ru(bpy)_3^{2+}$* in the presence of $Fe(CN)_6^{3-}$ and DNA from $w_0 = 10$ to $w_0 = 28$. The concentration of $Ru(bpy)_3^{2+}$ was the same for our experiments as it was for those of Atik and Thomas,[48] but our quencher concentration was half of that used by the latter, which accounts for our smaller overall quenching efficiency.

The low yield of emission quenching in AOT RMs can be explained by comparing the rate constant for quenching of $Ru(bpy)_3^{2+}$* to that for the spontaneous deactivation of $Ru(bpy)_3^{2+}$*, because these two pathways compete. In water, the quenching rate constant is 3.2×10^{10} M^{-1} s^{-1} and the rate constant for $Ru(bpy)_3^{2+}$* decay is 1.7×10^6 s^{-1} (on the basis of $Ru(bpy)_3^{2+}$* $\tau = 600$ ns).[64] Using these rate constants and a quencher concentration of 1 mM, we calculated the fraction of $Ru(bpy)_3^{2+}$* quenched in water to be 95%, which is very similar to the 85−90% we obtain in buffer solution. In contrast, at $w_0 = 22$ and 1 mM $Fe(CN)_6^{3-}$, the calculated first-order quenching rate constant for 50 μM $Ru(bpy)_3^{2+}$* interacting with one quencher molecule in a water pool is 6.5×10^6 s^{-1}.[48] This rate constant is larger than the intrinsic deactivation rate constant of $Ru(bpy)_3^{2+}$* in RMs (1.54×10^6 s^{-1}) by only a factor of 4.[48] If we assume that the concentration of excited states is the same in both media, a reasonable assumption when the same concentration of $Ru(bpy)_3^{2+}$ is used, and that the quenching efficiency is proportional to the fraction of excited states that produce the cage complex [Ru^{3+}···Q^-], the relative yield of G oxidation detectable by PAGE is the ratio of the quenching efficiencies in buffer and RMs. This ratio led us to expect about a 2-fold higher yield of oxidatively generated damage at G in buffer solution compared to that in RMs.

Quantification of the extent of oxidatively generated products in ^{32}P-labeled oligonucleotides by $Ru(bpy)_3^{3+}$ using high-resolution PAGE[7,9,58,65−69] indicates that the yield of

(63) Hubig, S. M.; Rodgers, M. A. J. *J. Phys. Chem.* **1990**, *94*, 1933.
(64) Chu, D. Y.; Thomas, J. K. *J. Phys. Chem.* **1985**, *89*, 4065.
(65) Gaspar, S. M.; Schuster, G. B. *J. Am. Chem. Soc.* **1997**, *119*, 12762.
(66) Ly, D.; Sanii, L.; Schuster, G. B. *J. Am. Chem. Soc.* **1999**, *121*, 9400.
(67) Kan, Y.; Schuster, G. B. *J. Am. Chem. Soc.* **1999**, *121*, 10857.

piperidine-labile G oxidation products is 1.6-fold lower for duplex **1** in RMs than in buffer solution. This decrease is consistent with the factor of 2 difference predicted from quenching efficiencies (see preceding paragraph). However, the cleavage ratio for single-stranded **1** in buffer solution vs RMs is higher by a factor of 13, which cannot be explained exclusively by a quenching efficiency argument.

One explanation for the low yield of oxidatively generated damage at G observed for single-stranded **1** in RMs is that Ru^{3+} oxidation of G does not compete effectively with charge-recombination reactions between reduced quencher and Ru^{3+} or $G^{\bullet+}$. The recombination rates between $Ru(bpy)_3^{3+}$ and reduced quencher in the presence of DNA or between $G^{\bullet+}$ and $[Fe(CN)_6]^{2-}$ have not been measured; however, it has been observed that the quencher identity affects the quantum yield of oxidatively generated damage at G in duplex DNA with the intercalating ruthenium polypyridyl complex $[Ru(phen)_2dppz]^{2+}$.[9] Thus, increased rates of recombination between reduced quencher and Ru^{3+} or $G^{\bullet+}$ in single-stranded **1** are a possible means to account for the lower-than-expected yield of piperidine-labile lesions in RMs.

Alternatively, the reaction manifold that guanine enters after oxidation in RMs might be different from that in dilute solution. The type of oxidative lesion generated depends on many factors, but the key step at which the chemistry differentiates for one-electron oxidants is after the formation of $G^{\bullet+}$.[7] Deprotonation of $G^{\bullet+}$ followed by the addition of O_2 leads to piperidine-labile products.[70] The addition of water to $G^{\bullet+}$ can ultimately lead to 8OG if followed by oxidation or 2,6,-diamino-4-hydroxy-5-formamidopyrimidine (FapyGua) if followed by reduction.[71,72] These products are not piperidine-labile and thus are not detectable using denaturing PAGE.[7] Further, if 8OG is formed, it can be oxidized by Ru^{3+} to yield the oxidation products spiroiminodihydantoin or guanidinohydantoin.[74−77] Production of the 8-hydroxy-7,8-dihydroguanyl radical (the precursor to 8OG and FapyGua) requires that water addition to $G^{\bullet+}$ compete with deprotonation to form $G^{\bullet}$. If the reaction of $G^{\bullet+}$ in single-stranded **1** with water is diffusion-controlled, a pseudo-first-order rate constant of approximately 5×10^{10} s^{-1} can be calculated. From pulse radiolysis experiments, the rate constant for $G^{\bullet+}$ deprotonation has been measured to be 1.8×10^7 s^{-1} for deoxyguanosine at pH 7; a similar rate constant is reported for duplex oligonucleotides.[73] These calculations predict that the dominant follow-up chemistry for $G^{\bullet+}$ in dilute solution should be formation of the 8-hydroxy-7,8-dihydroguanyl radical. It is not possible to predict which pathway dominates in RMs because the rate of water addition to $G^{\bullet+}$ will be different in the RM environment. Thus, our current studies that are underway to identify the products of oxidatively generated damage at G in RMs by HPLC-MS are important.[7,78−81]

Another explanation for the low yield of PAGE-detected guanine oxidation products in single-stranded **1** in RMs is a change in the solvent accessibility of guanine. The relative rates of one-electron G oxidation and recombination reactions are affected by the structure of the DNA substrate.[9,41,47,58,82−89] We observe a structural change when single-stranded **1** is incorporated in RMs. The hypochromicity of single-stranded **1** in RMs indicates increased base-stacking relative to that for single-stranded **1** in buffer solution, and the CD spectrum of single-stranded **1** in RMs is consistent with rigidification.[38] Thus, it is likely that guanines in single-stranded **1** are less accessible to the Ru^{3+} oxidant in RMs than in buffer solution, resulting in the decreased yield of oxidatively generated products in RMs. This explanation is consistent with results for duplex **1** as well. The structure of duplex **1** is unchanged in RMs;[23] therefore, the yield of piperidine-labile G oxidation products depends only on the relative quenching efficiencies of Ru^{2+}* in buffer vs RM solutions.

In addition to the difference in the yield of PAGE-detected G oxidation products observed across media for the same substrate, single- and double-stranded **1** exhibit differences in the same medium. In buffer solution, the levels of G oxidation detected by PAGE in single-stranded and duplex **1** parallel reported rate constants for G oxidation in dilute solution.[42,45,90] In RMs, comparable yields of G oxidation products are obtained for single-stranded and duplex **1**, indicating that the RM environment prevents guanine oxidation in the single-stranded DNA substrate.

In conclusion, our data point to a dramatic change in the conformation of single-stranded DNA in the anionic RM environment, leading to a decrease in the oxidative susceptibility of guanine. A variety of DNA-binding agents, including small molecules and proteins, protect guanine from

(68) Carter, P. J.; Cheng, C.-C.; Thorp, H. H. *J. Am. Chem. Soc.* **1998**, *120*, 632.
(69) Nunez, M. E.; Noyes, K. T.; Gianolio, D. A.; McLaughlin, L. W.; Barton, J. K. *Biochemistry* **2000**, *39*, 6190.
(70) Cadet, J.; Berger, M.; Buchko, G. W.; Joshi, P. C.; Raoul, S.; Ravanat, J.-L. *J. Am. Chem. Soc.* **1994**, *116*, 7403.
(71) Kasai, H.; Yamaizumi, Z.; Berger, M.; Cadet, J. *J. Am. Chem. Soc.* **1992**, *114*, 9692.
(72) Ravanat, J.-L.; Saint-Pierre, C.; Cadet, J. *J. Am. Chem. Soc.* **2003**, *125*, 2030.
(73) Kobayashi, K.; Tagawa, S. *J. Am. Chem. Soc.* **2003**, *125*, 10213.
(74) Luo, W.; Muller, J. G.; Rachlin, E. M.; Burrows, C. J. *Org. Lett.* **2000**, *2*, 613.
(75) Hah, S. S.; Kim, H. M.; Sumbad, R. A.; Henderson, P. T. *Bioorg. Med. Chem. Lett.* **2005**, *15*, 3627.
(76) Niles, J. C.; Wishnok, J. S.; Tannenbaum, S. R. *Chem. Res. Toxicol.* **2004**, *17*, 1501.
(77) Slade, P. G.; Hailer, M. K.; Martin, B. D.; Sugden, K. D. *Chem. Res. Toxicol.* **2005**, *18*, 1140.
(78) Cai, Z.; Sevilla, M. D. *Radiat. Res.* **2003**, *159*, 411.
(79) Ye, Y.; Muller, J. G.; Luo, W.; Mayne, C. L.; Shallop, A. J.; Jones, R. A.; Burrows, C. J. *J. Am. Chem. Soc.* **2003**, *125*, 13926.
(80) McCallum, J. E.; Kuniyoshi, C. Y.; Foote, C. S. *J. Am. Chem. Soc.* **2004**, *126*, 16777.
(81) Slade, P. G.; Hailer, M. K.; Martin, B. D.; Sugden, K. D. *Chem. Res. Toxicol.* **2005**, *18*, 1140.
(82) Odom, D. T.; Dill, E. A.; Barton, J. K. *Chem. Biol.* **2000**, *7*, 475.
(83) Kan, Y.; Schuster, G. B. *J. Am. Chem. Soc.* **1999**, *121*, 10857.
(84) Breslin, D. T.; Schuster, G. B. *J. Am. Chem. Soc.* **1996**, *118*, 2311.
(85) Sistare, M.; Holmberg, R.; Thorp, H. *J. Phys. Chem. B* **1999**, *103*, 10718.
(86) Lewis, F. D.; Letsinger, R. L.; Wasielewski, M. R. *Acc. Chem. Res.* **2001**, *34*, 159.
(87) Santhosh, U.; Schuster, G. B. *Nucleic Acids Res.* **2003**, *31*, 5692.
(88) Abdou, I. M.; Sartor, V.; Cao, H.; Schuster, G. B. *J. Am. Chem. Soc.* **2001**, *123*, 6696.
(89) Schuster, G. B. *Acc. Chem. Res.* **2000**, *33*, 253.
(90) Weatherly, S. C.; Yang, I. V.; Thorp, H. H. *J. Am. Chem. Soc.* **2001**, *123*, 1236.

oxidatively generated damage, presumably by prohibiting access of the oxidant or inhibiting follow-up chemistry.[25,26,35,91−96] In AOT RMs, the DNA is not expected to bind directly to the RM headgroups because both are negatively charged. Thus, AOT RMs protect guanines from damage through an indirect mechanism in which a structural change of the DNA is induced by its inclusion in the RM interior. Significant structural changes have been reported for single-stranded deoxyoligonucleotides in anionic liposomes in the presence of cations.[97] These cations were proposed to mediate adsorption of DNA on the anionic headgroups of the liposomes,[97] and a similar structural change might be occurring in our system. Further work is currently underway to test this hypothesis with a variety of cations and in RMs composed of positively charged surfactants.

Acknowledgment. Acknowledgment is made to the donors of the Petroleum Research Fund, administered by the American Chemical Society, for partial support of this research. This work also is supported by a NSF CAREER award to V.A.S. (CHE-0346066). Transient absorption experiments were conducted by Ms. Sun McMasters. Helpful suggestions and critical reading of the manuscript prior to submission by Ms. Kathleen Daugherty, Dr. Lisa Kelly, and Dr. David H. Stewart are gratefully acknowledged.

Supporting Information Available: Circular dichroism spectrum of DNA with $Ru(bpy)_3^{2+}$ in RMs, emission spectra of $Ru(bpy)_2dppz^{2+}$ in AOT RMs. This material is available free of charge via the Internet at http://pubs.acs.org.

IC0521022

(91) Wagenknecht, H.-A.; Stemp, E. D. A.; Barton, J. K. *J. Am. Chem. Soc.* **2000**, *122*, 1.
(92) Johansen, M. E.; Muller, J. G.; Xu, X.; Burrows, C. J. *Biochemistry* **2005**, *44*, 5660.
(93) Rajski, S. R.; Kumar, S.; Roberts, R. J.; Barton, J. K. *J. Am. Chem. Soc.* **1999**, *121*, 5615.
(94) Nunez, M. E.; Holmquist, G. P.; Barton, J. K. *Biochemistry* **2001**, *40*, 12465.
(95) Nguyen, K. L.; Steryo, M.; Kurbanyan, K.; Nowitzki, K. M.; Butterfield, S. M.; Ward, S. R.; Stemp, E. D. A. *J. Am. Chem. Soc.* **2000**, *122*, 3585.
(96) Stemp, E. D. A.; Barton, J. K. *Inorg. Chem.* **2000**, *39*, 3868.
(97) Patil, S. D.; Rhodes, D. G. *Nucleic Acids Res.* **2000**, *28*, 4125.